Space and Time Scales of Global Tropospheric Moisture

DIAN J. GAFFEN,*,@ TIM P. BARNETT** AND WILLIAM P. ELLIOTT*

*Air Resources Laboratory, National Oceanic and Atmospheric Administration, Silver Spring, Maryland
@Department of Meteorology, University of Maryland, College Park, Maryland
**Climate Research Division, Scripps Institution of Oceanography, La Jolla, California

(Manuscript received 22 February 1990, in final form 5 February 1991)

ABSTRACT

Radiosonde data from a global 118-station network are used to determine the spatial and temporal scales of variability of tropospheric water vapor. Various sources of possible error and bias in the data are analyzed. Changes in instrumentation at U.S. stations are shown to have a considerable influence on the record; information on comparable changes in other countries is not readily available. Mean monthly data are shown to be acceptable at tropical stations but not at high-latitude stations, where the nonlinear dependence of saturation vapor pressure on temperature, coupled with large temperature ranges, leads to biases of up to 10% in mean monthly specific humidity.

A series of three empirical orthogonal function analyses (for the tropics, North America, and the globe) of specific humidity at the surface, 850-mb, 700-mb, and 500-mb levels is presented. All three show evidence of a shift in the specific humidity field in the winter of 1976/77, with generally lower values from the beginning of the record (January 1973) until the shift and higher values through the winter of 1985/86. This shift is shown to be consistent with other evidence for a change in "climate state" in about 1977. The influence of the El Niño–Southern Oscillation is evident in both the tropical and global analyses.

1. Introduction

Tropospheric water vapor plays a principal role in the global climate system. Its direct radiative effects coupled with its indirect involvement in climate processes through cloud, aerosol, and chemical feedback mechanisms make water vapor a key element in the climate system. Because of its importance, the mean properties of the global moisture field have received considerable attention. For instance, climatological mean water vapor distributions have been fairly well characterized in previous analyses of aerological data from the global radiosonde network (e.g., Bannon and Steele 1960; Peixoto and Oort 1983). Mean water vapor transport and flux divergences have been computed to elucidate the role of atmospheric moisture in the global general circulation and hydrological cycle (e.g., Rasmusson 1972; Rosen et al. 1979).

In part because of predictions of increases in tropospheric water vapor associated with increasing atmospheric concentrations of carbon dioxide and other "greenhouse" gases (e.g., Mitchell 1989), several investigators have attempted to study the temporal variability of water vapor. Trenberth et al. (1987), using variations in total atmospheric pressure as an indicator of water vapor changes, found that the noise level in the model-analyzed fields was large enough to mask both interannual variability and trends in their 1978–85 dataset. Using monthly mean data from about 25 radiosonde stations in the tropics for the period 1965–84, Hense et al. (1988) estimated the precipitable water (PW) in the 700- to 500-mb layer using data from those two levels. Noting that this layer contains only about 20% of the total column water vapor content, the authors found a majority of the stations exhibit increases in both PW and relative humidity (RH) over the 20-year record. We shall see in section 3 that their calculated changes may have been influenced by instrumental error. Also possibly influenced by changes in practices and instrumentation is a study, similar to ours, by Salstein et al. (1983), who examined the modes of variability of annually averaged Northern Hemisphere water vapor for the period 1958–73. Flohn and Kapala (1989) used surface data (from the Comprehensive Ocean Atmosphere Data Set) from tropical oceanic regions for the period 1949–79 to determine trends in temperature, winds, and moisture content there. Using the saturation deficit between the sea surface and air as the primary moisture indicator, they found increases in nearly all of the regions selected for study. The trends were significant at the 95% confidence level for only one region, called the "warmest oceans," between 10°S and 10°N and between 60°E and 180°. Elliott et al. (1991) report preliminary results showing

Corresponding author address: Ms. Dian J. Gaffen, Air Resources Laboratory, NOAA/R/E/AR, SSNC2 Room 9358, 1325 East West Highway, Silver Spring, MD 20910.

an increase in the surface to 500-mb PW content in the Northern Hemisphere tropical atmosphere between 1973 and 1986.

While previous studies of tropospheric water vapor using radiosonde data have identified climatological means, and, to a lesser extent, long-term trends, little attention has been paid either to the reliability of the radiosonde data or to the natural variability of the tropospheric moisture field. Assessment of both is critical to future identification of long-term changes in water vapor. This paper investigates each of these sources of "noise" in the radiosonde record of tropospheric water vapor. Section 2 describes the available archived data and includes a discussion of potential pitfalls in their use. Section 3 estimates possible errors and biases in calculating monthly and longer term statistics. Section 4 addresses the time and space scales of variability of tropospheric water vapor and presents the results of a series of empirical orthogonal function (EOF) analyses of monthly average water vapor data from the archive. In section 5 we interpret the results of the EOF analyses in terms of interdecadal and interannual climatic variations. Section 6 concludes with an assessment of the utility of radiosonde data for detecting variations and change in tropospheric water vapor content.

2. The water vapor record in the radiosonde data archive

Our main source of information about the troposphere has been the global network of radiosondes launched generally twice daily to supply data needed for weather forecasts. Jenne and McKee (1985) describe the radiosonde data available in the archive and some of their attendant problems. The balloon-borne instruments, including the humidity sensors, vary from country to country and from manufacturer to manufacturer and have changed over the years. The World Meteorological Organization (WMO) catalogs 21 different radiosonde instrument types in use by its members in 1986 (WMO 1986), and there have been several changes in the humidity instruments used on radiosondes since the first sondes were flown in 1937 (U.S. Weather Bureau 1964). Table 1 lists some of the changes in the U.S. radiosonde system of which we are currently aware. Unfortunately, no equivalent historical information is now available for other countries, although the WMO Commission on Instruments and Methods of Observation (CIMO) recently resolved to conduct such a study for the benefit of climate researchers.

Two main problems account for much of the systematic error associated with radiosonde humidity measurements: slow response at low temperatures and hysteresis at very high and very low relative humidities (WMO 1983). When the number of water molecules in the air is very small, the response of many instruments is poor. Since saturation vapor pressure decreases rapidly with temperature (Fig. 1), low temperatures are associated with low vapor concentrations and poor instrument performance. According to the WMO (1983), "(f)rom about −20° to −40°C the [moisture] indications are useful only as qualitative information and at lower temperatures still most elements must be regarded as virtually useless." Some sensors, such as goldbeater's skin, used in British instruments, and electrolytic resistor elements, have particular problems when wetted by rain or very wet fogs (WMO 1983).

In a series of WMO-sponsored international radiosonde intercomparisons, Nash and Schmidlin (1987) found that RH measurements by most of the instruments tested tend to have a reproducibility, as estimated by the standard deviation of the measurement, of about 3.5%. An exception was the Indian lithium chloride hygristor, which had reproducibilities at approximately 7% for temperatures between 0° and 20°C and 17% for temperatures between −20° and −40°C. Temperature measurements tended to be reproducible to 0.2° to 0.4°C. Time constants for RH ranged from about 1 s for the carbon hygristors to several minutes for goldbeater's skin and hair hygrometers at high altitude. Carbon hygristors have lower sensitivity at low

TABLE 1. Changes in United States radiosonde instruments and practices that may influence humidity.

Date	Change and source of information
1943	Lithium chloride humidity element replaced the hair hygrometer (U.S. Weather Bureau 1964)
1948	Began computing all relative humidities (RH) using saturation values with respect to water. Prior computations involved saturation with respect to ice for temperatures below 0°C (U.S. Weather Bureau 1964; Lott 1976).
1962–65	Introduced carbon humidity element. Began reporting low RH measurements. (Earlier practice with lithium chloride sensor was not to report low values when the instrument was said to be "motorboating.") (Lott 1976).
1972	Redesigned relative humidity ducts introduced to reduce insolation effects on instrument that were responsible for low biases in RH measurements for some daytime sounding (Friedman 1972).
1973	Introduced current practice of considering measured RH less than 20% as "motorboating" and reporting all lower RH values as 19% (Wade and Wolfe 1989).
1980/81	New carbon hygristors introduced. Relative humidity transfer equation changed for the new sensor (Facundo, personal communication, 1989).

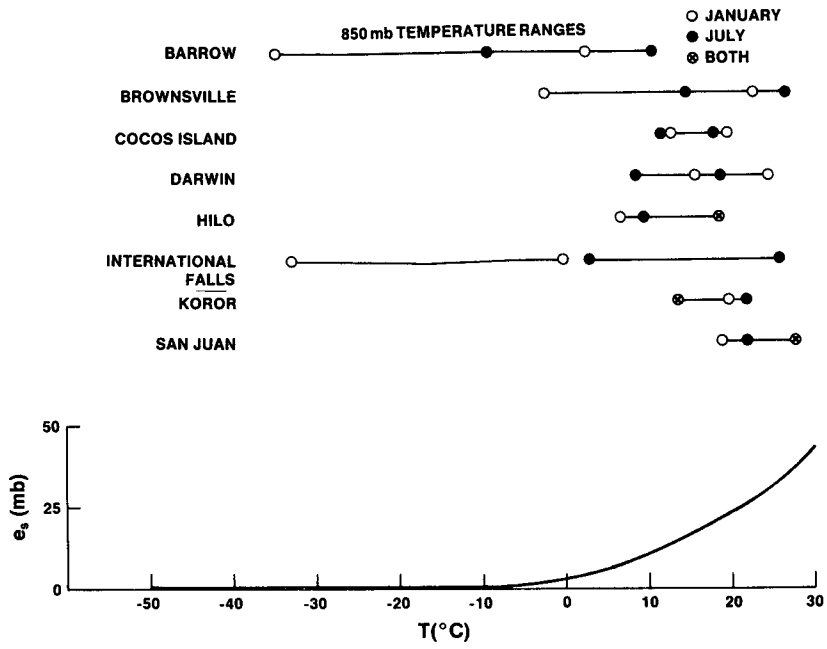

FIG. 1. Saturation vapor pressure (mb) as a function of temperature (°C) and typical January and July 850-mb temperature ranges at selected stations.

RH than at high RH, and the data from Australian and U.S. instruments have especially poor resolution for RH <20%. The Finnish thin-film capacitor, on the other hand, reports RH as low as 5%, but it reports values about 17% higher than carbon hygristors when "wetted." In summary, this intercomparison of a handful of contemporary instruments showed clearly that there are differences in performance characteristics among the various sensor types that lead to inhomogeneities in the data quality of the global dataset and that at high altitudes moisture data are unreliable. Unfortunately, little is known about the comparative performance of instruments in use before the 1980s.

The data employed in this study were obtained from the National Oceanic and Atmospheric Administration's (NOAA) National Climatic Data Center (NCDC) and from the National Center for Atmospheric Research (NCAR). The NCDC data are generally twice daily observations and cover the period 1973–1986 for the approximately 60-station network utilized by Angell and Korshover (1983) and described by Elliott et al. (1991). We shall refer to this group of data as dataset A. One set of NCAR data, derived from 29 different sources, including 13 NCDC datasets, also included daily observations, and we will refer to this as dataset B. Two criteria determined the selection of stations in this NCAR dataset—length of record and location; tropical stations were of prime interest. In addition, a second NCAR set (dataset C) was obtained, which consisted of mean monthly rawindsonde data ("CLIMAT" reports) derived from reports published in "Monthly Climatic Data of the World." The composite dataset (A, B, and C), which we refer to as the Cooperative Water Vapor Dataset, is summarized in the Appendix and station locations are shown in Figs. 5, 10, and 14.

3. Estimates of errors and biases in statistics based on radiosonde data

Studies of seasonal, interannual, and decadal changes in tropospheric water vapor require averaging individual radiosonde soundings from the archive or using previously computed monthly average data. This section addresses the main sources of random error and bias in computing statistics of radiosonde data, including: obvious errors in the reported data; inconsistent reporting of moisture variables, especially in cold and dry environments; sampling problems; distinctions between daytime and nighttime soundings; and bias introduced in using monthly average data due to the nonlinear relationships among moisture variables.

a. Obvious errors in the reported data

Working with both the data archives and the soundings from NMC, we encountered and later screened several types of obvious errors in the data, of which other users should be aware.

1) Reported surface pressures are sometimes unreasonably high. Temperatures aloft are sometimes unreasonable compared with long-term mean values.

2) High-altitude stations occasionally report mandatory level data at 1000 or 850 mb even though their

surface pressure is lower than one or both of those values.

3) Sometimes data at a given pressure level appear as both a mandatory and significant level, and they are not always consistent.

4) Occasionally we find more daily reports per month than there are days in the month. Errors of this sort were a nuisance but were readily removed from the dataset.

b. Differences in reporting of moisture variables

Some records obviously contain relative humidity as the moisture variable (much of dataset B), whereas others report dewpoint depression (datasets A and C and some records in dataset B). As there is a range of values for which these two variables can be confused, the issue is not trivially resolved.

Changes in instruments and reporting practices from country to country and over time (such as those listed in Table 1 for the United States) pose a second problem. For example, in the individual soundings from some stations we distinguish at least three periods of different reporting practices. Before 1965 RH values less than 21% are not found in the record, although the reports include values between −12 and −15. We interpret these negative values as some sort of code, although its meaning is not explained in any of the literature we have reviewed. From 1966–72 we find values of RH between 10% and 20%, but from 1973 to the present no values, positive or negative, less than 19 are found, and 19 is interpreted as a code for "motorboating." (The term "motorboating" was used in the early years of radiosonde operation when an audible "putt-putt-putt" was associated with low ordinate values on the relative humidity scale and dry conditions.) These interpretations are consistent with the changes listed in Table 1 and with Angell et al. (1984) who demonstrated the effect of the 1965 change on the interpretation of the records from two U.S. stations. Unfortunately, the rules cannot be applied globally as not all nations made the same changes. Rather than consider these codes as missing data, we converted all "motorboating" codes (30.0°C dewpoint depression, 19% relative humidity, etc.) to a nominal 15% relative humidity. To consider motorboating reports as missing would be to bias the data toward moist values. Substituting a fixed, low value of RH tends to correct this bias.

Table 1 includes changes in radiosonde instruments and practices that are documented in the literature and whose effects can be reasonably well judged, at least qualitatively. The first five changes listed justify our choice of 1973 as the beginning of our analysis period. The sixth entry regarding the introduction of new hygristors in 1980/81 is included because it may well have an impact on the humidity data, but at this time that impact is not clear. It is possible that the introduction of the new hygristor had some small effects, but a rather extensive literature search and discussions with radiosonde experts in the National Weather Service and elsewhere have yet to uncover them. More important, an examination of individual time series of moisture variables from U.S. stations has not revealed any sharp changes coincident with the introduction of the new hygristor at the stations. Therefore, we feel that at this time it is reasonable to assume that the change from one type of carbon hygristor to another did not have a large impact on the data.

c. Sampling problems

For the EOF analyses presented in section 4 we employed deviations from long-term mean monthly values for each station. To compute the means, a sufficient number of soundings were required for the month. Student's t-test specifies that

$$t = \frac{(\bar{x} - \mu)N^{1/2}}{s} \tag{1}$$

where $\bar{x}$ is the sample mean, μ the population mean, N is the number of observations, and s is the sample standard deviation. Working with specific humidity as the main variable of interest, we use the approximation

$$s \approx \frac{\bar{x}}{C} \tag{2}$$

where C is a constant whose value, estimated directly from the data, is typically 20. (This estimate is probably high for the near-surface layers and low for the upper troposphere.) Equations (1) and (2) imply that at least three observations per month are required to obtain an estimate of the monthly mean that falls within the 0.10 confidence bands. Since the stations were selected in part because of their reliable reporting, this lower limit was rarely reached, and estimates of monthly means have generally much higher confidence levels.

If two or fewer observations were available for a given month, the monthly mean was considered missing. More than 95% of the station months met the criterion. If one or two consecutive monthly means were missing, we linearly interpolated a value using the anomalies for the preceding and following months. Three or more consecutive months of missing data were given climatological mean values; i.e., deviations were set to zero.

d. Daytime versus nighttime soundings

Because radiosonde moisture instruments respond to ambient relative humidity rather than, for example, number density of water molecules, temperature effects on the instrument and its housing can be important. Indeed, Morrissey and Brousaides (1970) demonstrated that solar radiation penetrating the relative humidity duct of U.S. radiosonde instrument packages

resulted in biased humidity readings: measured RH was lower than ambient RH. Introduction of a new duct design in 1972 (Freidman 1972) corrected the problem. Whether other nations' instruments have had similar, radiation-induced problems, and whether they have been corrected, we do not know.

The record from Hilo, Hawaii, illustrates the potential impact of mixing day- and nighttime soundings in one analysis if there is a radiation error. Illustrated in Fig. 2 are mean monthly 850-mb level RH values from 1950 to 1987. The top panel shows mean values, smoothed by application of a five-point running mean, and includes soundings for 1200 UTC only. The bottom panel shows the difference in mean monthly RH between 1200 UTC and 0000 UTC soundings. From about 1965 to 1972 the 0000 UTC (daytime) RH values at 850 mb are markedly lower than the 1200 UTC (nighttime) values but before 1965 and after 1972 the difference is not noticeable. In February 1965 the radiosonde hygristors used at Hilo were changed from the lithium chloride type to the carbon element. The apparent 15%–25% difference in daytime soundings is likely due to penetration of solar radiation into the instrument housing, which was corrected by the new housing design, introduced in May 1972 at Hilo.

To avoid bias in monthly mean specific humidity at mandatory pressure levels, we selected 1973 as the beginning of our data record, thus, avoiding the 1972 change in U.S. radiosonde housing. (We recognize, however, that it may be possible to correct for the day–night differences at U.S. stations on a station-by-station basis, and that doing so would allow analysis of a longer record.) Nevertheless, day–night differences in specific humidity, due either to diurnal atmospheric changes or to instrumental problems, may remain. To assess these differences we selected six stations, identified in the Appendix and geographically distributed to represent a variety of climate types, for analysis. Their longitudinal distribution ensures that some take soundings near local noon and midnight and others launch closer to sunrise and sunset. Mean monthly specific humidity was computed from 0000 and 1200 UTC soundings, separately for each station, for each month and for each of the four levels: the surface, 850 mb, 700 mb, and 500 mb. Means were computed for a five-year period selected to avoid any known changes in radiosonde instrumentation and practices at each site, based on station histories provided by Barry Schwartz (personal communication).

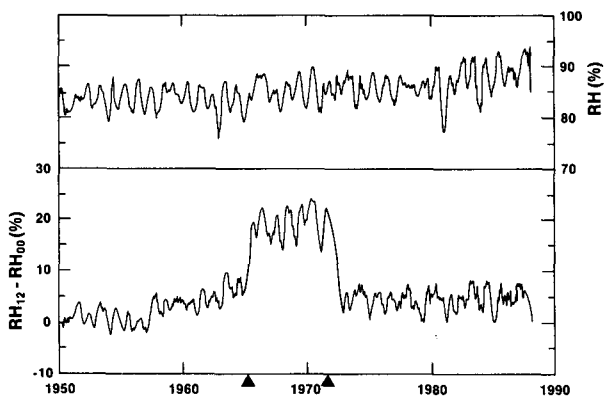

FIG. 2. Top panel: Five-month running mean of monthly average 850-mb 1200 UTC relative humidity (%) at Hilo. Bottom panel: difference in mean monthly relative humidity evaluated using 1200 UTC and 0000 UTC soundings from Hilo (1200 UTC–0000 UTC), also treated with five-month running mean. Arrows indicate introduction of carbon hygristor (February 1965) and change in instrument housing (May 1972).

In general, the difference between the 0000 and 1200 UTC means was less than 1% in magnitude and variable in sign. At Barrow, where specific humidity is low and solar effects are negligible on a 12-hour scale, differences were generally less than 0.1%. At Brownsville and Koror, differences as large as −4% were computed for individual months, but only at the surface, where they are likely to represent real diurnal changes in low-level moisture content associated with mesoscale processes such as sea-breeze circulations. Thus, we conclude that day–night differences in mean monthly specific humidity introduce a random error generally less than 1% in absolute magnitude.

Nevertheless, to avoid introducing the error into our dataset, we used nighttime soundings as much as possible. For a number of stations, the archives (datasets A and B) contained only daytime soundings, which were used in the analysis, so at least the resulting time series are self-consistent. For the mean monthly data (dataset C), the observation time was not known, and the data were accepted as given. At other stations all data were included in computing monthly means. The choice of observation time is listed in the Appendix. Thus the analysis is not for a fixed universal time. It is hoped that by using deviations from station means in our EOF analysis, any possible bias in a given station's daytime measurements will be minimized. Unrealistic horizontal structure due to instrument differences from one station to another will also be reduced.

e. Nonlinear relationships among moisture variables

In an early study of global water vapor climatology, Bannon and Steele (1960) recognized several sources of systematic error, apart from the heterogeneity of the observations, in the computation of mean monthly precipitable water from mean monthly radiosonde data. The most significant errors were attributed to 1) vertically integrating specific humidity to obtain precipitable water using only the mandatory pressure level data, and 2) calculating mean water vapor mixing ratios from mean dewpoint. (The error in converting mean mixing ratios to mean specific humidity was considered negligible.)

As this study does not involve vertical integration of precipitable water, our main source of bias due to

data manipulation will be in converting the mean monthly upper-air data (dataset C), where dewpoint, T_d, is the reported variable, to mean monthly specific humidity for analysis. The major source of bias is the nonlinear relation between relative humidity, RH, vapor pressure, e, and temperature, T.

We define the bias Δ as

$$\Delta = \tilde{e} - \bar{e} \tag{3}$$

where $\tilde{e}$ is the monthly mean vapor pressure computed from previously averaged monthly data, and $\bar{e}$ is the monthly mean vapor pressure based on daily vapor pressures computed from daily observations.

The bias can be estimated (A. Taylor, personal communication) as

$$\Delta = \frac{1}{2}\frac{\partial^2 e}{\partial x^2}\sigma_x^2 + \frac{1}{2}\frac{\partial^2 e}{\partial y^2}\sigma_y^2 + \frac{\partial^2 e}{\partial x \partial y}\sigma_x \sigma_y r_{x,y} \tag{4}$$

where e is a function of the independent variables x and y, the σ are their respective standard deviations, and $r_{x,y}$ is their correlation coefficient. We consider two cases: one in which e is a function of the single independent variable T_d, the dewpoint, such that e is the saturation vapor pressure, e_s, evaluated at T_d:

$$e = e_s(T_d) \tag{5}$$

and a second where e depends on both T and RH

$$e = e_s(T)\mathrm{RH}. \tag{6}$$

For case 1 we obtain

$$\Delta_1 = \frac{1}{2}\left(\frac{\partial^2 e_s(T_d)}{\partial T_d^2}\right)\sigma_{T_d}^2 \tag{7}$$

which is always negative, according to the Clausius–Clapeyron equation relating saturation vapor pressure and temperature:

$$\frac{\partial e_s(T_d)}{\partial T_d} = \frac{L e_s}{R_v T_d^2} \tag{8}$$

where L is the latent heat of vaporization (assumed constant) and R_v is the gas constant for vapor. Because the second derivative is negative, the mean e_s is underestimated by using the mean dewpoint. The magnitude of the second derivative is inversely proportional to the square of T_d, and the fractional error can be greater than 10% and as high as 20% in some cases at low temperatures (Elliott et al. 1991).

For case 2, since the second term on the right-hand side of (4) vanishes, we find

$$\Delta_2 = \frac{1}{2}\left(\frac{\partial^2 e_s(T)}{\partial T^2}\right)\sigma_T^2(\mathrm{RH}) + \frac{\partial e_s(T)}{\partial T}\sigma_T \sigma_{\mathrm{RH}} r_{T,\mathrm{RH}}. \tag{9}$$

The first term in (9) is always negative, but the second takes the sign of the correlation between the daily T and RH values. To determine the magnitude and sign of this term, we selected eight stations, indicated in the Appendix, for analysis. Mean monthly specific humidity values at the four levels defined above were computed both correctly, using daily specific humidities, and incorrectly, using mean monthly temperature and relative humidity. Five-year periods were selected, and the monthly means were separately calculated for each observation time. In addition, the correlation coefficient between temperature and relative humidity for each level, observation time, and month over the five-year period was computed. Table 2 summarizes the average computed bias, Δ_2, as a percentage of the true mean monthly value, $\bar{e}$.

At tropical stations, the bias is typically positive and of order one percent. At Brownsville, biases are positive except at the surface and have magnitudes of 2% to 3%, and at the high-latitude stations, the incorrect method yields 5% to 10% underestimates of mean monthly specific humidity. The small positive values at tropical stations imply that the error is due to noise in the data since we find negative correlations between T and RH. That the values at high-latitude stations are large and negative suggests that the second term in (9) is either small and positive or is negative in order to be consistent with a negative correlation between temperature and relative humidity.

The actual correlation coefficients between T and RH were computed from the daily data for the same five-year period used to compare daytime and nighttime data in section 3d. Using five years of data for each monthly correlation coefficient, we had a nominal 150 pairs of data (30 observations per month for 5 years) for each calculation. The correlations were limited to a five-year data period to avoid known changes in instrumentation and practices that might influence (tend to exaggerate) the correlation. These correlation coefficients were generally significant (exceeding 0.14, the 0.05 level) and almost always negative regardless of observation time, month, or level in the atmosphere, with typical values of -0.2 to -0.5 and a few as large as -0.8. We can conclude that the small positive biases computed for the tropical stations are due to noise in

TABLE 2. Average ratio of computed bias in mean monthly specific humidity based on monthly mean data to mean value derived from daily observations, $\Delta/\bar{e}$ (%).

Station	Latitude	Level			
		Surface	850 mb	700 mb	500 mb
Barrow	71.2°N	−9.5	−3.7	−4.5	−4.7
Internat. Falls	48.3°N	−10.3	−5.0	−6.1	−8.1
Brownsville	25.5°N	−2.6	+2.6	+2.9	+1.5
Hilo	19.4°N	−0.2	+0.2	+4.3	+1.2
San Juan	18.5°N	0.0	+0.6	+2.9	+1.6
Cocos Island	12.1°N	−0.1	+0.3	+0.8	+0.1
Koror	7.3°N	+0.2	+0.4	+1.3	+0.8
Darwin	12.4°S	−0.7	+0.3	+0.9	+0.8

the data, whereas the negative values at higher latitudes are a result of the combined effect of the curvature of the saturation vapor pressure function and the negative correlation between T and RH.

The latitudinal distribution of the bias follows from the nonlinearity of the Clausius–Clapeyron equation, and the within-month temperature variance. Figure 1 shows typical January and July 850-mb temperature ranges at each of the eight sample stations as well as the dependence of saturation vapor pressure on temperature. For the five low-latitude stations, temperature ranges are about 10°C, and over that range the saturation vapor pressure curve can be reasonably approximated by a line segment, so the use of monthly average T and RH to estimate specific humidity is a good approximation. However, at higher latitudes, temperature ranges are several times larger, especially in winter, and are associated with substantial curvature in the saturation vapor pressure relation, and linearity is a poor assumption.

We conclude that significant negative correlations between daily temperature and relative humidity observations augment the potential bias in computing monthly average specific humidity from monthly average temperature and relative humidity. At tropical stations, the bias is smaller than the noise in the data, which is likely to result in about a 1% overestimate of mean specific humidity. However, at high-latitude sites, where large temperature ranges accentuate the problem of nonlinearity between temperature and saturation vapor pressure, this effect dominates and a 5% to 10% underestimate can result. Based on this result, we accepted mean monthly data (dataset C) from tropical stations within 30° latitude of the equator for inclusion in our analyses.

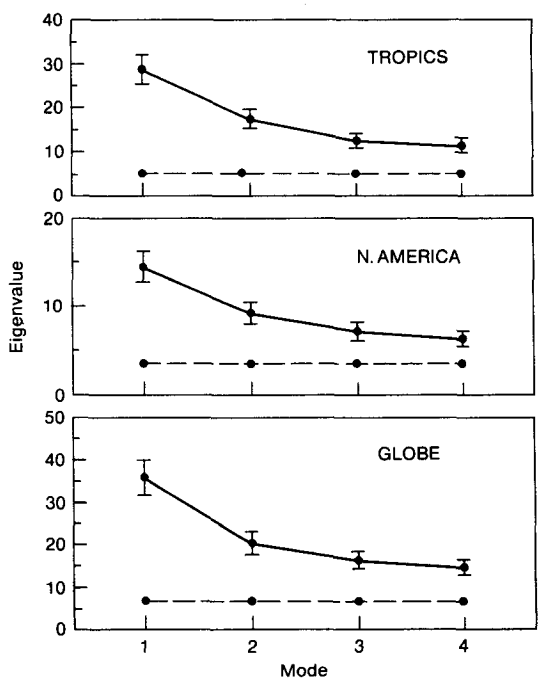

FIG. 3. Eigenvalues and their error bars, computed following North et al. (1982), and Rule N 90% confidence levels for the first three modes of each EOF analysis. Top, middle, and bottom panels are for the tropical, North American, and global analyses, respectively.

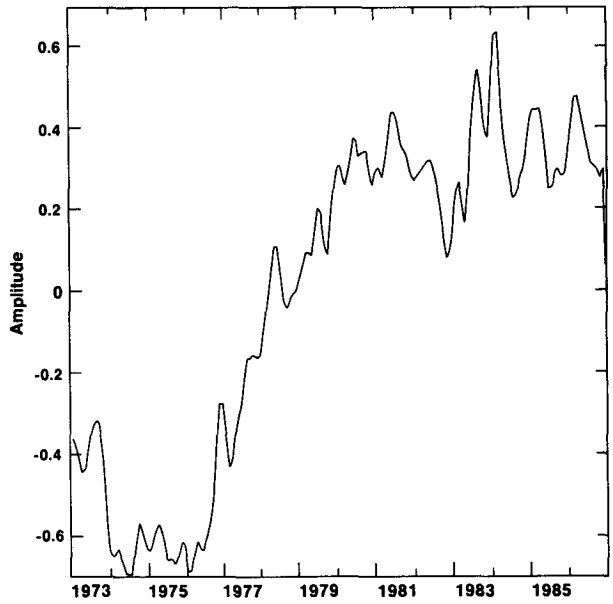

FIG. 4. Amplitude function for mode 1 of the tropical specific humidity EOF analysis. Large tick marks indicate January of odd-numbered years. Values have been smoothed with a 1–4–6–4–1 filter. This mode explains 11.3% of the total variance. The product of an amplitude function and its associated eigenvector will have units of standard deviations.

4. Empirical orthogonal function analyses of radiosonde data

Using mean monthly specific humidity at each of four levels (surface and 850, 700, and 500 mb) over the 168-month period January 1973 through December 1986, three empirical orthogonal function (EOF) analyses were performed to elucidate the time and space scales of variations in atmospheric moisture content. A global study used data from all 118 sites. Because of the strong interannual atmospheric changes known to occur in the tropical atmosphere, a separate tropical analysis, incorporating data from the 76 stations between 30°N and 30°S latitude, was made. And because of the high density and quality of radiosonde data over North America, the 33 stations in that region were also treated separately. Appendix A indicates the stations comprising each dataset.

For each analysis, mean monthly specific humidity anomalies (deviations from the long-term mean for that month) for the four levels were concatenated to form a single anomaly array. The resulting amplitude

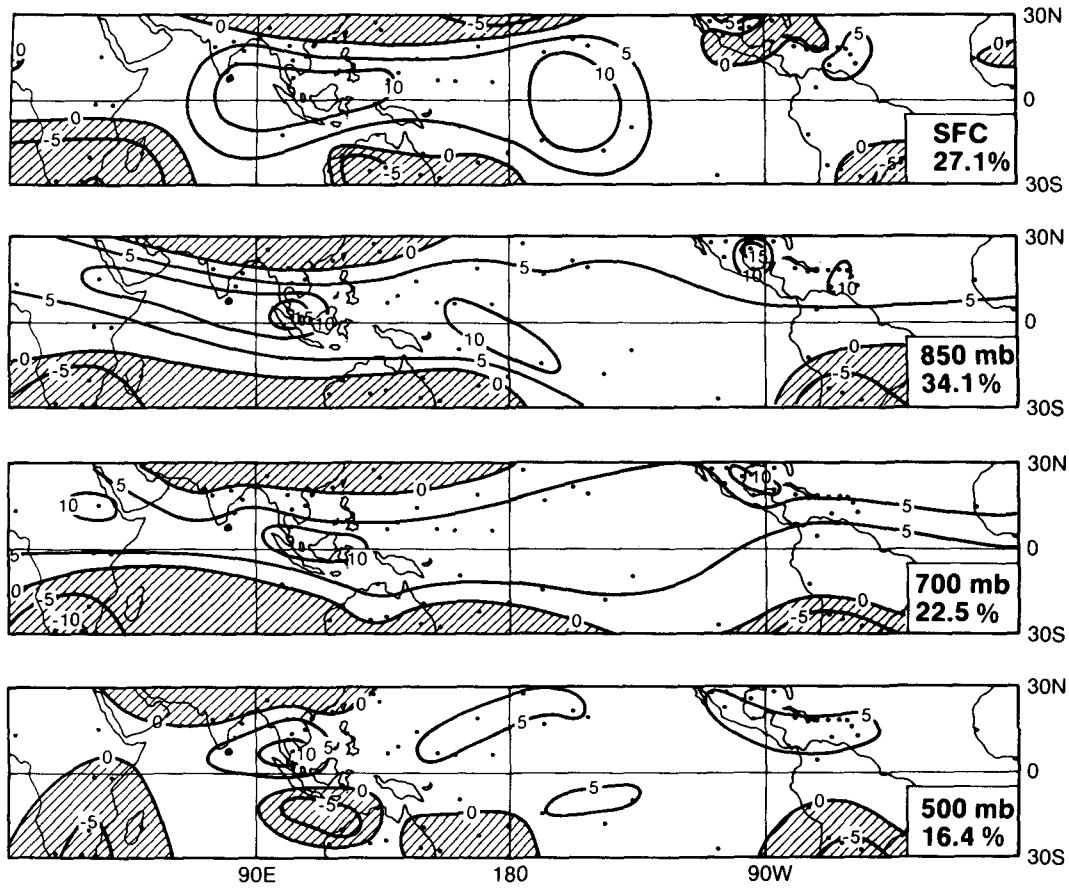

FIG. 5. Eigenvector pattern for mode 1 of the tropical specific humidity EOF analysis. Dots represent station locations, and regions of negative values are shaded. The panels represent, from top to bottom, the surface, 850-mb, 700-mb, and 500-mb levels. Boxed numbers in the corners are the fractional variance associated with each level.

functions thus describe the simultaneous temporal behavior of the specific humidity of the four levels (cf. Barnett and Hasselmann 1979). Correlation matrices were used, and the product of the amplitude function and eigenvector gives the sign and magnitude (in number of standard deviations) of local anomalies. The 0.10 significance level of individual eigenvalues was determined by Rule N (Preisendorfer 1988). For fields of Gaussian random values, an eigenvalue would exceed this level only once in ten experiments. Following North et al. (1982) we then distinguish only those modes for which the difference between successive eigenvalues is statistically distinct. The eigenvalues, their associated error bars, and Rule N 90% confidence levels for the first three modes of each analysis are shown in Fig. 3. In each of the three runs, the first two modes were significant and distinguishable, although for the global analysis, the second mode just barely met the North et al. criterion. Amplitude functions associated with these modes were smoothed using a 1-4-6-4-1 filter for subsequent display. The following subsections briefly describe the results of the analyses and section 5 suggests a physical interpretation.

a. Tropical analysis

The first mode of the tropical analysis, which explains 11.3% of the total variance, has amplitude functions and eigenvectors as shown in Figs. 4 and 5. The amplitude functions exhibit a steplike change from negative to positive values in 1977 and remain positive through the end of the record. The eigenvector patterns are vertically consistent and are positive over the equatorial belt and negative toward the higher latitudes. Taken together, the eigenvectors and amplitude functions for this mode can be interpreted as an increase in specific humidity in the equatorial belt at each level from the 1973–77 period to the 1978–86 period. An investigation of the vertical eigenstructure of the specific humidity field showed that the largest fractional variance (34.1%) of this field is at the 850-mb level. The fractional variance associated with each level for each mode of each analysis, as well as the percent variance explained by each mode, is indicated in the eigenvector maps and the accompanying figure captions. In this analysis, as in the other two described below, the similarity of the eigenvector patterns at each of the

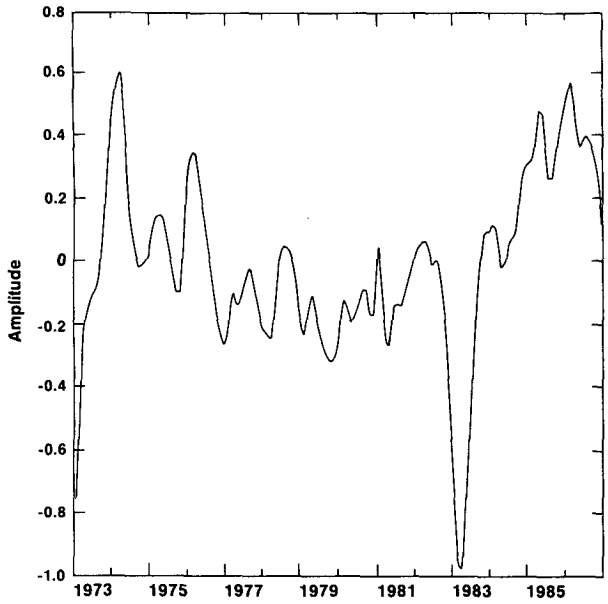

FIG. 6. Same as Fig. 4 but for mode 2 of the tropical specific humidity EOF analysis. This mode explains 5.8% of the total variance.

four levels, as well as the relatively even distribution of variance associated with each level, supports the notion of concatenating the four levels.

Mode 2 has a very different structure and explains 5.8% of the total variance. Figures 6 and 7 show the amplitude functions and eigenvectors, respectively. The amplitude functions fluctuate between positive and negative values, with large signals in early 1974, 1976, 1983, and 1985. The eigenvector map shows regions of positive and negative anomalies, the strongest signal being in the western Pacific, north of the equator and west of the date line, where positive regions are evident at all levels.

A time series of monthly values of the Southern Oscillation index is presented in Fig. 8 for comparison with the amplitude function. The correspondence between the two suggests that this second mode is associated with the El Niño–Southern Oscillation, which is the dominant climatic signal in the tropics. Negative values of the amplitude function during 1983 indicate that the air over the western Pacific was drier than usual during that strong El Niño, while the eastern Pacific, the Caribbean, and Southeast Asia were anomalously

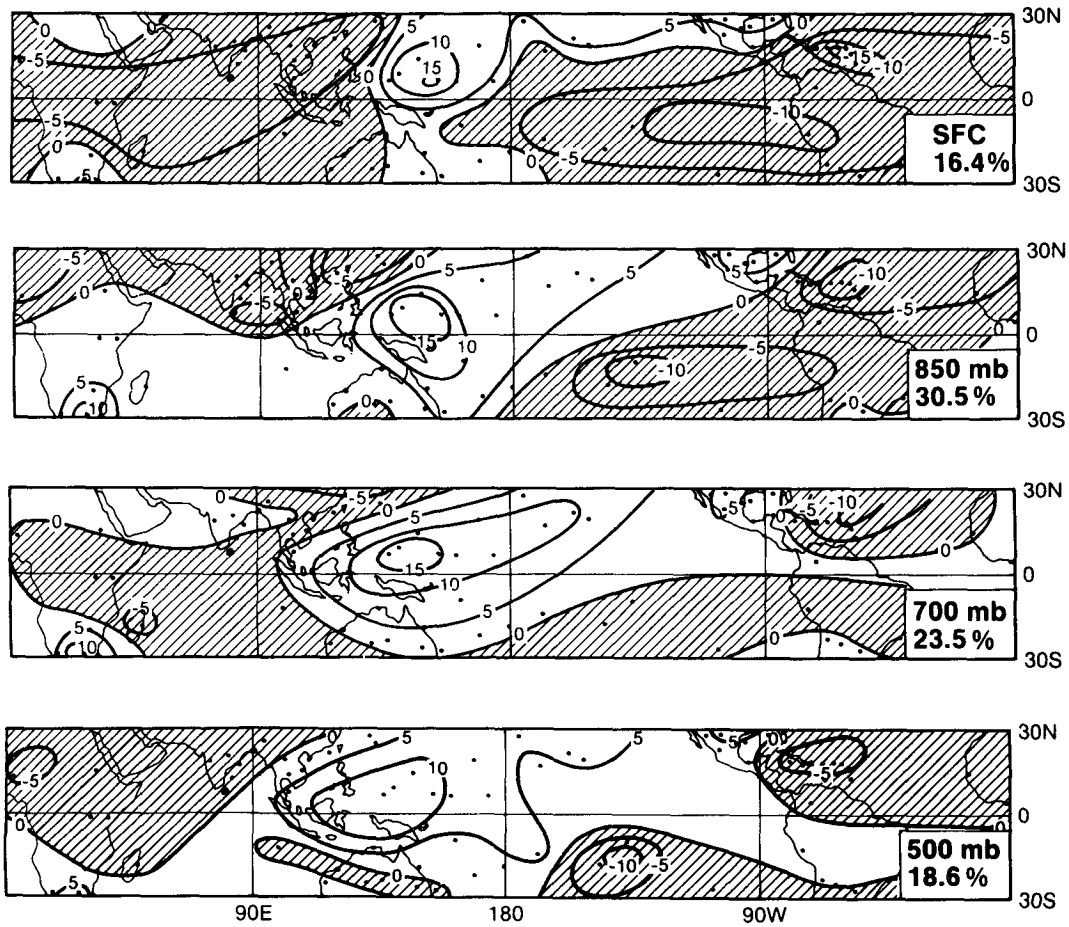

FIG. 7. Same as Fig. 5 but for mode 2 of the tropical specific humidity EOF analysis.

and North American stations account for 79% of the total global dataset. Since the results are not sensitive to changes in analysis domain, we are confident that they are not spurious artifacts of the analysis technique. The amplitude functions for mode 1, which explain 7.7% of the total variance, closely resemble those for mode 1 in both the tropics and North America and shift from negative to positive values in 1977 (Fig. 13). The associated eigenvector pattern is shown in Fig. 14 and is positive over large parts of the globe. There is a suggestion of a dipole in the pattern over the North Pacific, somewhat similar in structure to the eigenvector pattern presented by Prabhakara et al. (1985) for the second mode describing monthly deviations of precipitable water over the oceans, derived from satellite microwave radiometer data for 1979–1983.

The second mode of the global analysis explains 4.4% of the total variance and is just barely distinct, but we present it because of its similarity to the second mode of the tropical EOF analysis. The amplitude functions, shown in Fig. 15, are related to those of the second mode in the tropical analysis (Fig. 6), which were shown above to be closely related to the Southern Oscillation index. The correlation coefficient between the amplitude functions of this mode and the Southern Oscillation index is 0.34 ± 0.06 for the unfiltered values, which is greater than 0.16, the minimum value for a statistically significant correlation. The correlation for the filtered values is only slightly higher, 0.40 ± 0.05, which indicates the minimal effect of the filter. The spatial pattern for this mode (Fig. 16) shows the strongest response in the tropical western Pacific and over North America. The structure noted in mode 2 of the North American analysis, eigenvectors of opposite sign in the Caribbean and the continental United States, is evident here as well.

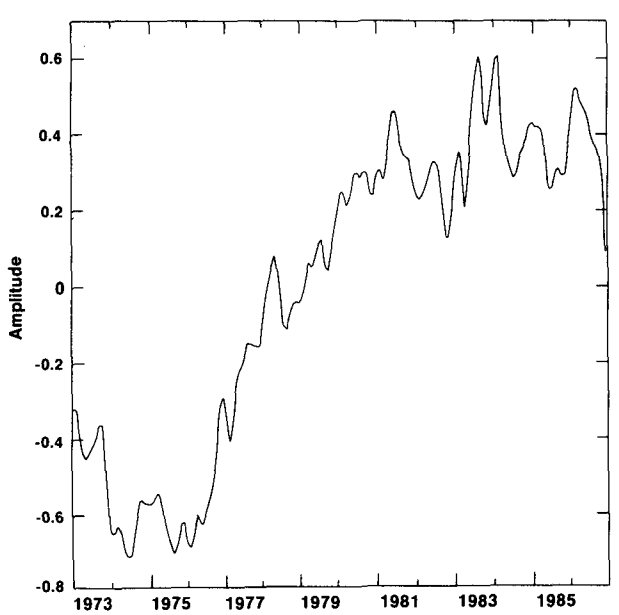

FIG. 13. Same as Fig. 4 but for mode 1 of the global specific humidity EOF analysis. This mode explains 7.7% of the total variance.

Both of the first two modes of the global analysis support the contention that the strongest signal in the tropospheric moisture field is at low latitudes, although our network is less dense at high latitudes, particularly in the Southern Hemisphere. However, the notion that the tropical region and extratropics have inversely related moisture variations, which our tropical analysis suggested, is not completely borne out by the global analysis.

d. Vertical structure of tropospheric moisture

The EOF analyses of tropospheric moisture content all showed that the largest relative change in moisture variance is associated with the 850-mb level. The greatly diminished quality of the radiosonde data at the 500-mb level and above make analysis of higher altitudes difficult. The eigenvector maps show more or less coherent pictures at each level for the tropical analysis (Fig. 5), but in the global and North American analyses there is more variation in the vertical (e.g., Fig. 10). That baroclinicity in the extratropics is evident in the moisture field is not surprising, which highlights the importance of attention to the vertical structure of moisture when studying climatic variability and long-term change.

5. Discussion

a. State transition: significance and direct causes

The time series of the first mode of specific humidity (q) for the tropical Pacific stations clearly suggests the existence of distinct "states" or regimes in the variables. We performed a separate EOF analysis of tropical air temperature (T) whose first mode, not shown, had a similar structure. The initial state (beginning of record to winter 1976/77) is characterized by lower T and q values while higher T and q values characterize the second period (winter 1976/77 to winter 1985/86). It appears the latter state came to an end in winter 1985/86 but that is near the end of the data record, so such a conclusion is tenuous at this time. The similarity of the T and q patterns strongly suggests that tropical moisture variations are related to temperature anomalies. This conclusion is also quantitatively consistent with the magnitudes of changes of T and q. We defer further discussion of this interesting relation here, but note that the analysis of Graham (1992) strongly suggests the origins of the signal are in the temperature changes in the tropical Pacific Ocean.

One immediately wonders if the apparent step change in specific humidity suggested by the amplitude functions of the first mode of the three EOF analyses are statistically significant. We investigated this point by selecting four stations (Yap, Truk, Koror, and Pon-

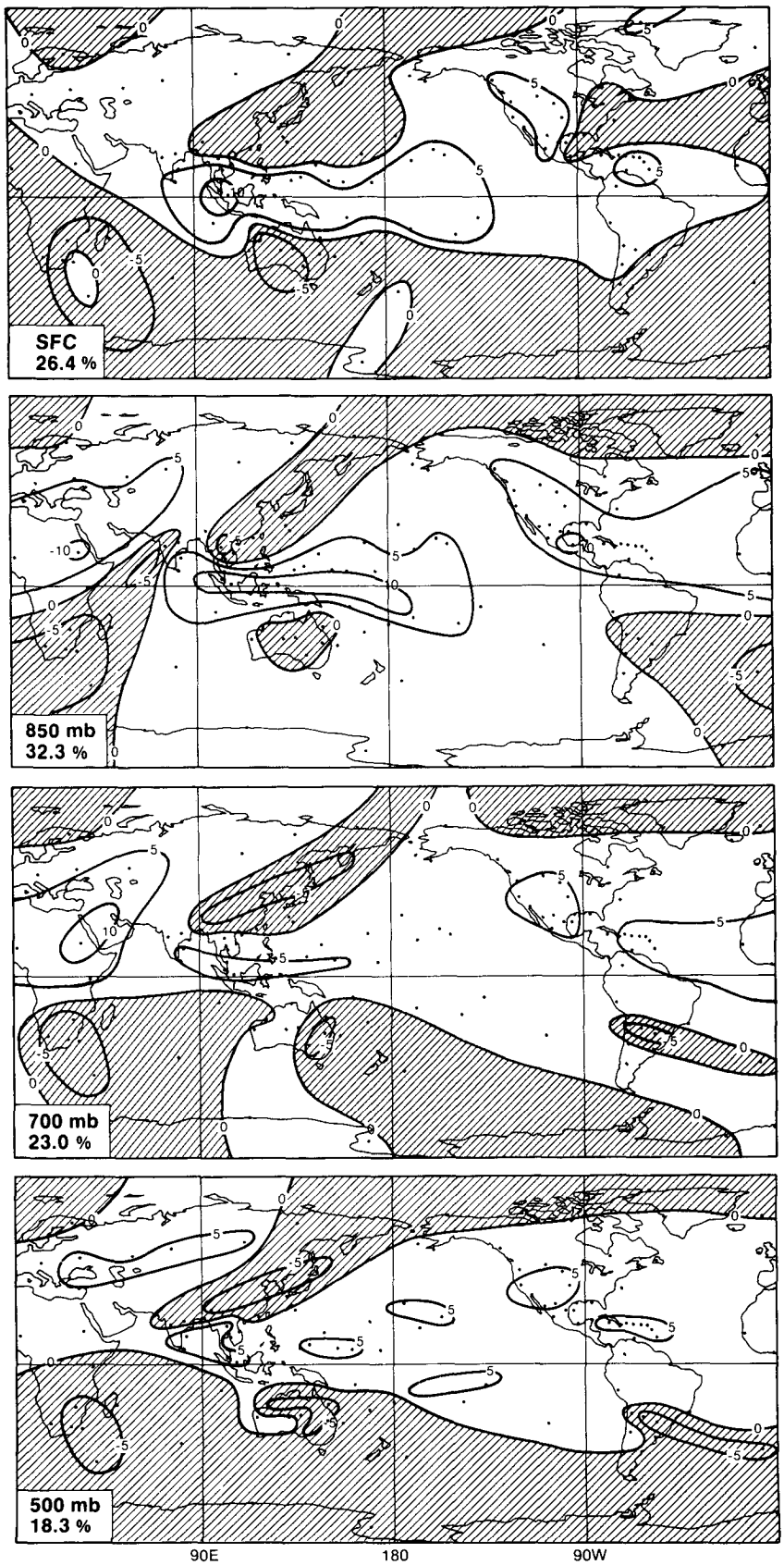

FIG. 14. Same as Fig. 5 but for mode 1 of the global specific humidity EOF analysis.

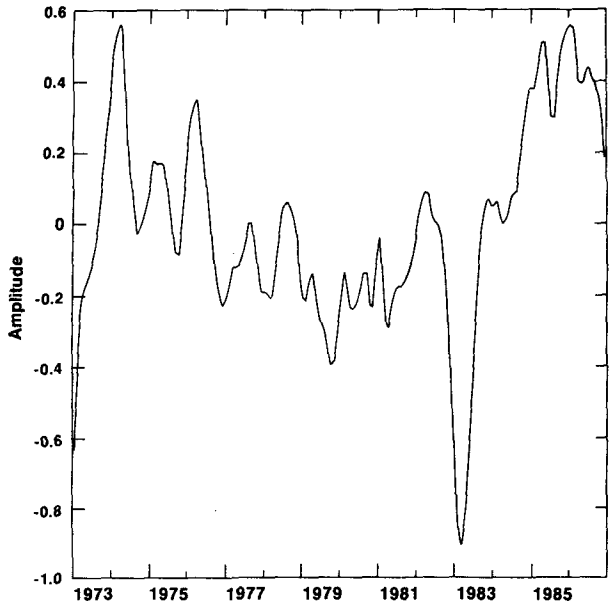

FIG. 15. Same as Fig. 4 but for mode 2 of the global specific humidity EOF analysis. This mode explains 4.4% of the total variance.

ape) at which the eigenvectors for that mode were large, indicating a strong signal, for closer study. We defined two periods, May 1974 to April 1976, and May 1980 to April 1982, one preceding and one following the 1977 step change in amplitude functions. Mean temperature, dewpoint, specific humidity, and relative humidity and their standard deviations over the two 24-month periods were computed and are shown in Table 3. Statistical significance was evaluated with the t test. These calculations were all made for the 850-mb level, which accounted for the largest fractional variance for that mode.

Increases in all four variables were noted at each of the four stations: Truk, Ponape, Koror, and Yap. The changes in the means were significant at least at the 95% level, except at Koror. To test the sensitivity of this result to the choice of time period, the analysis was repeated for the two periods May 1973 to April 1975 and May 1984 to April 1986, and the results were very similar, but the changes at Koror were statistically significant between these two periods. We conclude that the step function change in specific humidity is related to real increases in both temperature and relative humidity, since both variables changed significantly.

Time series of mean annual 850-mb specific humidity for the four stations are shown in Fig. 17. As measures of within-year variability, a typical value of the standard deviation of the monthly means over the course of a year is approximately 0.7 g kg^{-1}, as shown in Fig. 17. The annual cycle leads to a range of monthly values, which is typically about 3.0 g kg^{-1}. While there are some outlying points (in particular the 1983 value at Truk, for which we can find no satisfactory explanation), the increase in 850-mb specific humidity from the middle 1970s to the 1980s is evident.

As a final note, it would be of interest to extend the T and q sets back beyond 1973, looking for other apparent changes in regime. Unfortunately, the instrumental changes (noted earlier) in 1965 and 1972 show up dramatically and pose problems for the analysis of pre-1972 moisture data. For instance, Salstein et al. (1983) carried out a similar EOF analysis of radiosonde-derived moisture data for the 1958–73 period, using the precipitable water from the surface to 300 mb as their humidity variable. They found that only the first EOF was significant and was coherent over a large part of the globe. The tropical atmosphere divided into two regions showing contrasting behavior, with strongest signals over West Africa and in the western Pacific near the Caroline Islands. The associated time series suggested that the Pacific area became markedly drier, and the African area more moist, at about the middle of their record, that is, about 1964/65. Because this is the time when the United States introduced the new humidity element with its new housing and changed procedures to record drier observations, the apparent drying in the western Pacific—where many stations are operated by the United States—could be due to these changes alone.

b. *Evidence for shift of climate regimes*

The results of the prior section showed that a shift in regime is observed simultaneously in the T, RH,

TABLE 3. Mean 850-mb temperature, T (°C), dewpoint, T_d (°C), specific humidity, q (g kg^{-1}), and relative humidity, RH (%) at four tropical stations for May 1974–April 1976 (subscript 1) and for May 1980–April 1982 (subscript 2). Standard deviations are given in parentheses.

Station	T_1	T_2	T_{d1}	T_{d2}	q_1	q_2	RH_1	RH_2
Truk	17.8 (0.3)	18.5 (0.4)	13.3 (1.0)	14.5 (1.1)	11.1 (0.7)	11.9 (0.8)	75 (5)	78 (4)
Ponape	17.4 (0.4)	18.1 (0.4)	13.4 (0.8)	14.7 (0.8)	11.1 (0.6)	12.1 (0.6)	77 (4)	81 (3)
Koror	17.7 (0.4)	18.2 (0.4)	13.3 (1.1)	13.9 (1.7)	11.1 (0.8)	11.5 (1.2)	76 (5)	76 (8)
Yap	17.6 (0.4)	18.1 (0.5)	13.2 (1.1)	14.5 (1.5)	11.0 (0.8)	11.9 (1.2)	76 (5)	82 (3)
Average	17.6	18.2	13.3	14.4	11.1	11.9	76	79

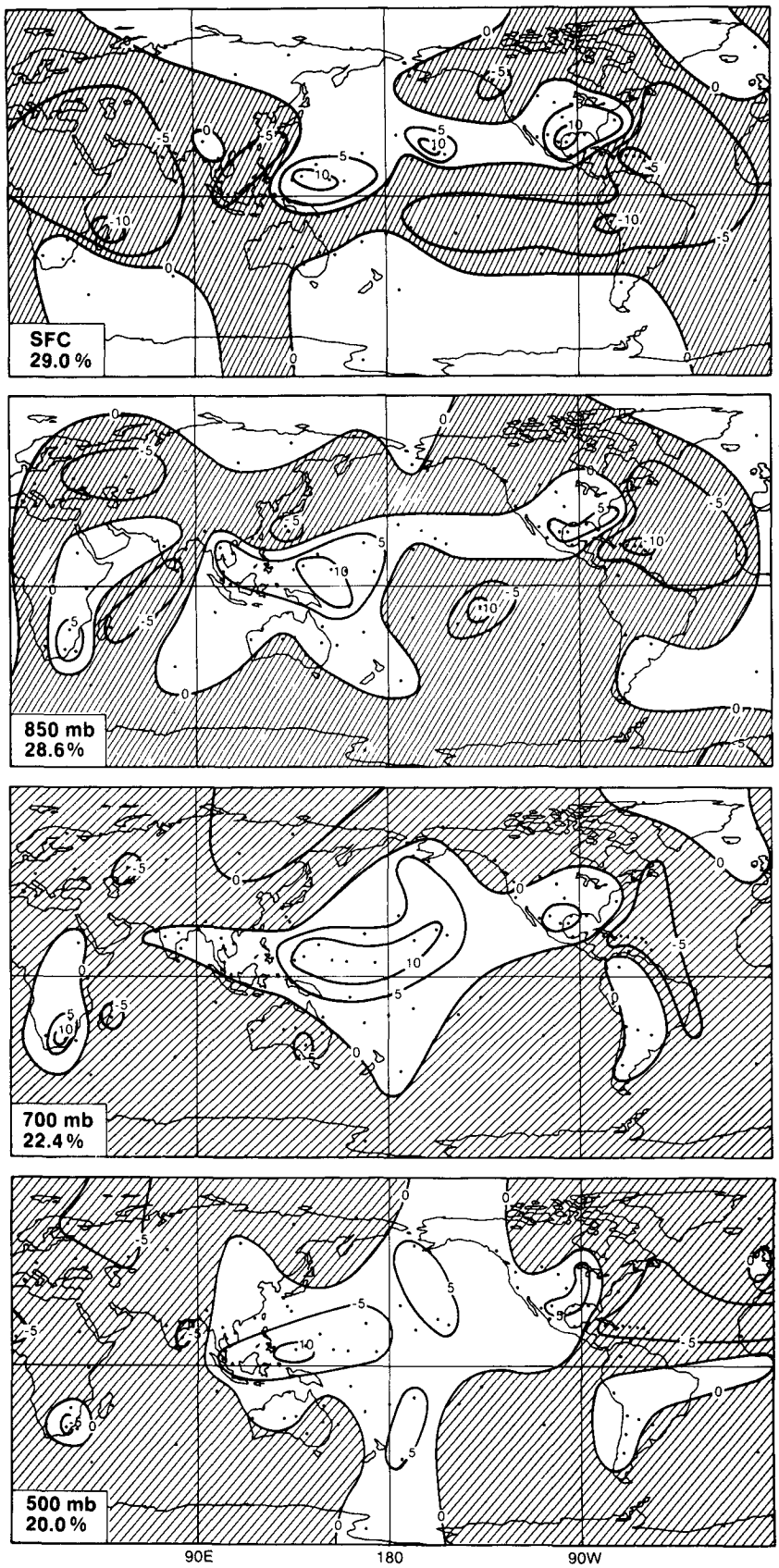

FIG. 16. Same as Fig. 5 but for mode 2 of the global specific humidity EOF analysis.

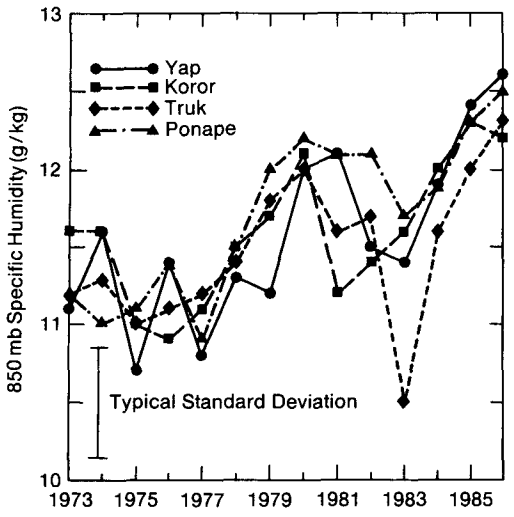

FIG. 17. Mean annual 850-mb specific humidity (g kg^{-1}) at four tropical stations from 1973 to 1986. The error bar represents a typical value of the standard deviation of the monthly means used to calculate the annual values.

and q field of the tropics and over North America. The commonality of the shift in these variables may signal a transition from one climate regime to another. There is a substantial, and growing, body of additional empirical evidence that also suggests a change of climatic regime in the 1976/77 period:

1) Venrick et al. (1987) show an abrupt steplike shift in the atmosphere (deepening of the Aleutian Low), ocean [colder than normal sea surface temperature (SST)], and fauna (increased phytoplankton) of the central North Pacific during the 1976/77 period.

2) Nitta and Yamada (1989) confirm the North Pacific SST changes found by Venrick et al. (1987) and show that the eastern tropical Pacific experienced an increase in SST between 1976 and 1977. An eigenvector analysis of global SST fields by Hsiung and Newell (1983) also supports this result.

3) Shabbar et al. (1988) show a similarly timed shift in the 500-mb height field with the largest signal (a decrease) over the North Pacific.

4) Folland and Parker (1988) show similar shifts in both North Pacific SST and in the air temperature over North America.

5) A similar transition is documented in the West Coast ocean swell climatology (Seymour et al. 1984); the frequency of extreme wave episodes increased after 1976, a result to be expected from the intensification of the Aleutian Low.

6) Trenberth (1990) reviews the changes noted above, pointing out that they are all dynamically consistent. He cites similar changes in the sea level pressure and surface wind stress field over the North Pacific and in the Southern Oscillation index as supporting the idea of a shift in regime in the 1976/77 time period.

All of the above evidence is consistent with the idea of a shift and/or amplification of the long-wave pattern over the North Pacific and North America. Evidence for such a shift following the 1976/77 winter is also presented by Graham (1992). However, Graham goes two steps further than the above authors:

1) He shows that the same type of shift in regime occurred in the SST field of the equatorial Pacific, with the post-1977 period being associated with higher SST (0.75°–1.0°C). Such values are quite comparable to those we have observed in the surface data of the tropical Pacific radiosonde stations.

2) The SST changes are shown to be related to increased convective activity in the tropics. This forcing, in turn, can explain most of the midlatitude features noted above, including the spatial distribution of change over the Pacific and North America, as well as the abrupt temporal shift. The increased convective activity is compatible with the increased values of q we found, because the main tropical precipitation patterns are essentially linearly proportional to q for temperatures above $\approx$27.5°C (Graham and Barnett 1987; Barnett et al. 1991).

In summary, the apparent shift in regime we have detected in the tropospheric temperatures and specific humidity appears not only statistically significant but also in accord with other tropical and extratropical data. The work of Graham (1992) suggests the genesis of the shift may well have been in the SST field of the central equatorial Pacific. Why this field changed in the first place is an open but vitally important question.

6. Conclusion

This paper has examined the spatial and temporal scales of variability in global tropospheric moisture as revealed by archived radiosonde data. We assessed the sources of error in using radiosonde humidity measurements for climate studies. The archive was found to contain certain obvious errors, which were easily removed, and inconsistencies, which we treated by applying some reasonable assumptions. We find that a minimum of three soundings per month are required to obtain reasonable monthly averages. Changes in radiosonde instruments over time can introduce bias into the dataset. In particular, at U.S. stations daytime data for the 1965–72 period are biased toward low humidities due to penetration of solar radiation into the instrument housing; therefore, we began our study period in 1973. Use of mean monthly data to compute mean monthly specific humidity is acceptable at tropical stations, where the bias introduced is less than 1% and apparently less than the noise level in the data. However, at high latitudes the nonlinear relationship among moisture variables, coupled with typically large temperature ranges, leads to biases of up to 10%.

Three empirical orthogonal function analyses

brought out several important aspects of the temporal and spatial scales of water vapor variations for the period 1973–86. In the tropics, over North America, and globally, we find the first mode to exhibit a steplike change in sign at about 1977. This result is consistent with previous work by other investigators who find evidence for a large-scale change in climate regime in 1977. The direction of this change is such that it describes a general increase in specific humidity in the tropics and over North America from the earlier period to the later. The second mode in the tropics and globally is closely related to the El Niño. For both modes, the water vapor signal is strongest in the tropics and at the 850-mb level. The eigenvector patterns are not exceedingly complex, which gives us confidence in the ability of the network to resolve important variations in water vapor.

Acknowledgments. The authors would like to thank Drs. James Angell and Alan Robock for helpful discussions, Mr. Tony Tubbs for computational assistance, and William Barnett for the crucial but tedious analysis of raw data. Work was partially supported by the Lawrence Livermore National Laboratory through the Department of Energy Grant DOE Contract W-7405-ENG-48, by the Climate Dynamics Division of the National Science Foundation through Grant ATM88-14571, and by the Scripps Institution of Oceanography. DJG will use part of this report in a Ph.D. dissertation at the University of Maryland.

APPENDIX

List of Stations

The following table lists the stations used in this study. The primary identifier is the WMO number. Positive (negative) values of latitude indicate Northern (Southern) Hemisphere locations. East (west) longitudes are given as postive (negative). Datasets A, B, and C are discussed in section 2 of the text. The group symbols indicate which stations comprise each EOF analysis. Group T is the tropical analysis, group N is the North American analysis, group B is both T and N, and group G is the global analysis. Stations included in groups T, N, and B were also included in the global analysis, as were stations in group G.

The observation time chosen for analysis is indicated by 1 for 0000 UTC, 2 for 1200 UTC, and 4 for either 0000 or 1200 UTC or both. The symbols to the left of the group symbols indicate stations that were used in special anlayses. The + indicates the analysis of day–night differences (section 3d) as well as the analysis of bias introduced by using mean monthly data (section 3e), and the * indicates the temperature-relative humidity correlation analysis (section 3e). The @ indicates the analysis of climate state transition (section 5a).

WMO number	Name	Latitude (deg)	Longitude (deg)	Dataset	Group	Observation time
01001	Jan Mayen	70.90	−8.70	A	G	4
02836	Sodankyla	67.40	26.70	A	G	4
03953	Valentia	51.90	−10.20	A	G	4
04018	Kevflavik	63.58	−22.36	B	G	2
10868	Munchen	48.10	11.70	A	G	4
20674	Ostrov Dikson	73.50	80.20	A	G	4
21965	Chetyrekhstolbovy	70.60	162.40	A	G	4
24266	Verkhoyansk	67.50	133.40	A	G	4
28698	Omsk	54.90	73.40	A	G	4
30230	Kirensk	57.80	108.10	A	G	4
33345	Kiev	50.40	30.50	A	G	4
35121	Orenburg	51.70	55.10	A	G	4
42410	Gauhati	26.10	91.70	C	T	4
42809	Calcutta	22.50	88.30	A	T	4
42867	Nagpur	21.10	79.10	C	T	4
43003	Bombay	19.10	72.80	A	T	4
43149	Vishakhapatnam	17.70	83.20	C	T	4
43279	Madras	13.00	80.20	C	T	1
43371	Trivandrum	8.50	77.00	A	T	4
45004	Hong Kong	22.30	114.20	A	T	4
47401	Wakkanai	45.40	141.70	A	G	4
47909	Naze	28.40	129.60	C	T	4
47945	Minami Daito Jima	25.80	131.20	C	T	4

WMO number	Name	Latitude (deg)	Longitude (deg)	Dataset	Group	Observation time
48327	Chiangmai	18.80	99.00	C	T	4
48407	Ubon	15.20	104.90	C	T	4
48455	Bangkok	13.70	100.50	C	T	4
48568	Songkhla	7.20	100.60	C	T	4
48601	Penang	5.30	100.30	C	T	4
48694	Singapore	1.30	103.90	A	T	1
61052	Niamey	13.50	2.20	A	T	4
61641	Dakar	14.70	−17.40	A	T	4
61996	Amsterdam Island	−37.80	77.60	A	G	4
62721	Khartoum	15.60	32.60	C	T	4
63741	Nairobi	−1.30	36.60	A	T	4
65578	Abidjan	5.20	−3.90	A	T	4
67083	Antananarivo	−18.80	47.50	A	T	4
67964	Bulwayo	−20.00	28.60	A	T	4
68406	Alexander Bay	−28.60	16.50	C	T	4
68442	Bloemfontein	−29.10	26.20	C	T	4
68588	Durban	−30.00	31.00	C	T	4
68906	Gough Island	−40.40	−9.90	A	G	4
68994	Marion Island	−46.90	37.90	A	G	4
70026	Barrow	71.30	−156.80	A	+, * N	2
70308	St. Paul Island	57.10	−170.20	A	N	2
70316	Cold Bay	55.12	−162.43	B	N	2
70398	Annette Island	55.00	−131.60	B	N	2
71072	Mould Bay	76.20	−119.30	A	N	4
71082	Alert	82.50	−62.30	A	N	4
71815	Stephenville	48.50	−58.60	A	N	4
71836	Moosonee	51.30	−80.60	A	N	4
72232	Boothville	29.00	−89.40	C	B	2
72250	Brownsville	25.90	−97.40	A	+, * B	2
72255	Victoria	28.90	−96.90	C	T	4
72290	San Diego	32.80	−117.70	B	N	2
72304	Cape Hatteras	35.16	−75.33	B	N	2
72451	Dodge City	37.46	−99.58	B	N	2
72493	Oakland	37.44	−122.12	B	N	2
72662	Rapid City	44.03	−103.04	B	N	2
72694	Salem	44.55	−123.01	B	N	2
72712	Caribou	46.52	−68.01	B	N	2
72747	International Falls	48.34	−93.23	B	+, * N	2
72775	Great Falls	47.50	−111.30	A	N	2
76225	Chihuahua	28.60	−106.10	C	B	4
76256	Empalme	27.90	−110.90	C	B	2
76394	Monterrey	25.70	−100.30	C	B	2
76458	Mazatlan	23.20	−106.40	C	B	4
76644	Merida	21.00	−89.50	C	B	4
76692	Veracruz	19.20	−96.10	C	B	1
78383	Grand Cayman	19.20	−81.40	C	B	2
78397	Kingston	17.90	−76.80	C	B	2
78486	Santo Domingo	18.50	−69.90	C	B	2
78526	San Juan	18.50	−66.00	A	+, * B	2
78866	St. Maarten	18.00	−63.10	C	B	2
78897	Guadeloupe	16.30	−61.50	C	B	4
78954	Barbados	13.10	−59.50	C	B	2
78988	Curacao	12.20	−69.00	C	B	2
80222	Bogota	4.60	−74.10	A	T	4
83746	Rio de Janiero	−22.80	−43.30	A	T	4

WMO number	Name	Latitude (deg)	Longitude (deg)	Dataset	Group	Observation time
84628	Lima	−12.01	−77.09	B	T	1
85442	Antofagasta	−23.50	−70.40	A	T	2
85469	Isla Pascua	−27.20	−109.40	A	T	4
85543	Quintero	−32.47	−71.32	B	G	2
85799	Puerto Montt	−41.50	−72.90	A	G	4
87047	Salta	−24.90	−65.50	C	T	4
87155	Resistencia	−27.50	−59.00	C	T	4
89001	S.A.N.A.E.	−70.30	−2.40	A	G	4
89022	Halley Bay	−75.50	−26.60	A	G	4
89564	Mawson	−67.60	62.90	A	G	4
89611	Casey	−66.30	110.60	A	G	4
89664	McMurdo	−77.80	166.60	A	G	4
91066	Midway Island	28.20	−177.40	C	T	2
91165	Lihue	22.00	¯159.30	C	T	2
91217	Guam	15.00	145.00	A	T	2
91245	Wake Island	19.30	166.70	A	T	2
91275	Johnston Island	17.30	−169.50	C	T	2
91285	Hilo	19.70	−155.10	A	+, * T	2
91334	Truk	7.50	151.90	C	@ T	4
91348	Ponape	7.00	158.20	C	@ T	4
91376	Majuro	7.10	171.40	A	T	4
91408	Koror	7.30	134.50	C	+, *, @ T	4
91413	Yap	9.50	138.10	C	@ T	4
91517	Honiara	−9.40	160.00	A	T	1
91592	Noumea	−22.30	166.50	C	T	4
91680	Nadi	−17.80	177.50	A	T	4
91765	Pago Pago	−14.30	−170.60	C	T	2
91925	Atuona	−9.80	−139.00	A	T	4
91938	Tahiti Island	−17.60	−149.60	A	T	4
93986	Chatham Island	−44.00	−176.50	A	G	2
94120	Darwin	−12.40	130.90	C	* T	1
94294	Townsville	−19.30	146.80	A	T	1
94300	Carnarvon	−24.90	113.70	C	T	1
94312	Port Hedland	−20.40	118.60	A	T	1
94326	Alice Springs	−23.80	133.90	C	T	1
94461	Giles	−25.00	128.30	C	T	4
94510	Charleville	−26.40	146.30	C	T	1
94578	Brisbane	−27.40	153.10	C	T	1
94672	Adelaide	−31.50	138.60	A	G	4
96996	Cocos Island	−12.10	96.90	A	* T	1

REFERENCES

Angell, J. K., and J. Korshover, 1983: Global temperature variations in the troposphere and stratosphere, 1958–1982. *Mon. Wea. Rev.*, **111**(5), 901–921.

——, W. P. Elliott and M. E. Smith, 1984: Tropospheric humidity variations at Brownsville, Texas and Great Falls, Montana, 1958–80. *J. Climate Appl. Meteor.*, **9**, 1286–1295.

Bannon, J. K., and L. P. Steele, 1960: Average water-vapour content of the air. *Geophys. Mem.*, No. 102, U.K. Meteorological Office, M.O. 631b, p. 38.

Barnett, T. P., and J. Hasselmann, 1979: Techniques of linear prediction with application to oceanic and atmospheric fields in the tropical Pacific. *Rev. Geophys. Space Phys.*, **17**, 949–968.

——, E. Kirk, M. Latif and E. Roeckner, 1991: On ENSO Physics. *J. Climate*, **4**, 487–515.

Elliott, W. P., M. E. Smith and J. K. Angell, 1991: Monitoring tropospheric water vapor changes using radiosonde data. *Greenhouse-Gas-Induced Climate Change:* A critical appraisal of simulations and observations. M. E. Schessinger, Ed., Elsevier, 311–327.

Flohn, H., and A. Kapala, 1989: Changes in tropical sea–air interaction processes over a 30-year period. *Nature*, **338**, 244–338.

Folland, C. K., and D. Parker, 1988: Observed variations of sea-surface temperature. *Proc. NATO Advanced Research Workshop in Climate–Ocean Interaction.* Oxford, M. E. Schlesinger, Ed., Kluwer, 21–52.

Friedman, M., 1972: A new radiosonde case: The problem and the solution. *Bull. Amer. Meteor. Soc.*, **53**(9), 884–887.

Graham, N., 1990: Interdecadal climate changes in the tropical Pacific and Northern Hemisphere 700 mb heights.

——, and T. Barnett, 1987: Sea-surface temperature, surface wind

divergence, and convection over the tropical oceans. *Science,* **238,** 657–659.

Hense, A., P. Krahe and H. Flohn, 1988: Recent fluctuations of tropospheric temperature and water vapour content in the tropics. *Meteor. Atmos. Phys.,* **38,** 215–227.

Hsiung, J., and R. E. Newell, 1983: The principal nonseasonal modes of variation of global sea-surface temperature. *J. Phys. Oceanogr.,* **13,** 1957–1967.

Jenne, R. L., and T. B. McKee, 1985: Data. Chapter 42, *Handbook of Applied Meteorology,* D. Houghton, Ed., John Wiley & Sons, 1461 pp.

Lott, G. A., 1976: Precipitable water over the United States, volume 1: Monthly means. NOAA Tech. Rep. NWS 20, 173 pp. Available from U.S. Department of Commerce, National Oceanic and Atmospheric Administration, National Weather Service.

Mitchell, J. F. B., 1989: The "greenhouse" effect and climate change. *Rev. Geophys.,* **27**(1), 115–139.

Morrissey, J. F., and F. J. Brousaides, 1970: Temperature-induced errors in the ML-476 humidity data. *J. Appl. Meteor.,* **9,** 805–808.

Nash, J., and F. J. Schmidlin, 1987: WMO International Radiosonde Intercomparison (U.K., 1984, U.S.A., 1985) Final Report, World Meteorological Organization, Instruments and Observing Methods Rep. No. 30, WMO/TD-No. 195, p. 103.

Nicholson, S. E., and B. S. Nyenzi, 1990: Temporal and spatial variability of SSTs in the tropical Atlantic and Indian Oceans. *Meteor. Atmos. Phys.,* **48,** 1–17.

Nitta, T., and S. Yamada, 1989: Recent warming of tropical sea-surface temperature and its relationship to the Northern Hemisphere circulation. *J. Meteorol. Soc. Japan.,* **67,** 375–383.

North, G. R., T. L. Bell, R. F. Cahalan and F. J. Moeng, 1982: Sampling errors in the estimation of empirical orthogonal functions. *Mon. Wea. Rev.,* **110,** 699–706.

Peixoto, J. P., and A. H. Oort, 1983: The atmospheric branch of the hydrological cycle and climate. *Variations in the Global Water Budget,* A. Street-Perrott, M. Beran and R. Ratcliffe, Eds., D. Reidel, 5–65.

Prabhakara, C., D. A. Short and B. E. Volmer, 1985: El Niño and atmospheric-water vapor: Observations from Nimbus 7 SMMR. *J. Climate Appl. Meteor.,* **24,** 1311–1324.

Preisendorfer, R., 1988: *Principal Component Analysis in Meteorology and Oceanography.* Elsevier Press, p. 425.

Rasmusson, E. M., 1972: Seasonal variation of tropical humidity parameters. *The General Circulation of the Tropical Atmosphere, Vol. 1,* R. E. Newell, Ed., MIT Press, 193–237.

Rosen, R. D., D. A. Salstein and J. P. Peixoto, 1979: Variability of large-scale atmospheric water vapor transport. *Mon. Wea. Rev.,* **107,** 26–37.

Salstein, D. A., R. D. Rosen and J. P. Peixoto, 1983: Modes of variability in annual hemispheric water vapor and transport fields. *J. Atmos. Sci.,* **40,** 788–803.

Seymour, R., R. Strange, D. Cayan and R. Nathan, 1984: Influence of El Niño on California's wave climate. *Proc. 19th Int. Conf. on Coastal Engineering,* Houston, Amer. Soc. Coastal Eng. 577–592.

Shabbar, A., K. Higuichi and J. Knox, 1988: Regional analysis of the secular variation of Northern Hemisphere 50-kPa heights. *Proc. 13th Annual Climate Diagnostics Workshop,* U.S. Dept. Commerce, NOAA, NWS, CAC, [Available from the National Tech. Info. Service. U.S. Dept. Commerce, 5285 Port Royal Road, Springfield, VA 22161.] 176–183.

Trenberth, K. E., J. R. Christy and J. G. Olson, 1987: Global atmospheric mass, surface pressure, and water vapor variations. *J. Geophys. Res.,* **92**(D12), 14 815–14 826.

Trenberth, K., 1990: Recent observed interdecadal climate changes in the Northern Hemisphere. *Bull. Amer. Meteor. Soc.,* **71,** 988–993.

U.S. Weather Bureau, 1964: History and catalogue of upper air data for the period 1946–1960. Key to Meteorological Records Documentation No. 5.21, U.S. Department of Commerce, Weather Bureau, Washington, D.C., 352 pp.

Venrick, E., J. McGowan, D. Cayan and T. Hayward, 1987: Climate and chlorophyll *a:* Long term trends in the central North Pacific. *Science,* **238,** 70–72.

Wade, C. G., and D. E. Wolfe, 1989: Performance of the VIZ carbon hygristor in a dry environment. *12th Conf. on Weather Analysis and Forecasting,* Monterey, CA, Amer. Meteor. Soc., 58–62.

World Meteorological Organization, 1983: *Guide to Meteorological Instruments and Methods of Observations,* Fifth edition, WMO-No. 8, 13.1–13.26.

World Meteorological Organization, 1986: *WMO catalogue of radiosondes and upper-air wind systems in use by members.* Instruments and Observing Methods Rep. No. 27, WMO/TD-No. 176.